Available online at www.sciencedirect.com
SCIENCE DIRECT®
Journal of Photochemistry and Photobiology A: Chemistry 169 (2005) 131–137
Journal of Photochemistry and Photobiology A:Chemistry
www.elsevier.com/locate/jphotochem

Dynamics of *E. coli* membrane cell peroxidation during TiO_2 photocatalysis studied by ATR-FTIR spectroscopy and AFM microscopy

V.A. Nadtochenko[a,*], A.G. Rincon[b], S.E. Stanca[a], J. Kiwi[a]

[a] *Laboratory of Photonics and Interfaces, Institute of Molecular Chemistry and Biology, EPFL, Lausanne 1015, Switzerland*
[b] *Laboratory of Biological Engineering, ENAC, Institute of Molecular Chemistry and Biology, EPFL, Lausanne 1015, Switzerland*

Received 13 May 2004; accepted 18 June 2004
Available online 31 July 2004

Abstract

Escherichia coli (*E. coli*) photokilling due to the TiO_2 under light irradiation in a batch reactor was studied by using of attenuated total reflection Fourier transform infrared spectroscopy (ATR-FTIR) and atomic force microscopy (AFM). The ATR-FTIR spectral features and AFM images were analyzed in relation to *E. coli* viability data. ATR-FTIR is shown to be a suitable technique to follow the structural changes of the *E. coli* cell membranes during TiO_2 photocatalysis. Formation of the peroxidation products due to the photocatalysis of *E. coli* cell is reported by this technique. Time dependent ATR-FTIR experiments provides the evidence for the changes in the *E. coli* cell wall membranes as the precursor events leading to bacterial lysis. Under the same experimental conditions used by ATR-FTIR spectroscopy, AFM microscopy was carried out to provide direct evidence for the *E. coli* lysis taking place under light irradiation after about 1 h in the presence of TiO_2. By transmission electron microscopy (TEM), the aggregated TiO_2 Degussa P-25 in aqueous solution is shown to interact with the bacteria surface and partly to remain in the aqueous solution at the concentration of 1 mg/ml.

Keywords: *E. coli* photokilling; TiO_2 photocatalysis; FTIR time dependent spectroscopy; *E. coli* lysis

1. Introduction

Investigations related to the abatement of toxic compound and bacteria in aqueous solutions using TiO_2 photocatalysis has been recently reported [1,2]. The abatement of bacteria, fungi and viruses by TiO_2 photocatalysis has been the subject of growing interest during the last decade but the photokilling mechanism is not well understood at the present time [12]. In this work we have selected Fourier transform infrared spectroscopy (FTIR) to obtain structural and conformational information during the TiO_2 photocatalyzed abatement of *E. coli* as it has been used during the last years in cell biology and medicine [1,4]. The aim of the current study is to report novel data by ATR-FTIR spectroscopy to monitor the chemical and structural changes due to *E. coli* peroxidation by TiO_2 photocatalysis. This study presents the bacterial cell wall changes induced by the TiO_2 photocatalysis followed by attenuated total reflection Fourier transform infrared spectroscopy (ATR-FTIR) and atomic force microscopy (AFM). To our knowledge it is the first application of ATR-FTIR to follow the *E. coli* bacterial cell wall structure changes within the time of TiO_2 photocatalysis leading to bacteria photokilling.

2. Experimental

2.1. Materials

TiO_2 Degussa P-25 ($50\,m^2/g$, 1 mg/ml) was used as a photocatalyst in aqueous suspension. A batch reactor

* Corresponding author. Tel.: +41 21 693 3162; fax: +41 21 693 4111.
E-mail address: john.kiwi@epfl.ch (V.A. Nadtochenko).

1010-6030/$ – see front matter © 2004 Elsevier B.V. All rights reserved.
doi:10.1016/j.jphotochem.2004.06.011

(Pyrex, 50 ml; Hanau Suntest solar simulator with a flux of 1000 W/m^2) during the photocatalytic runs with continuous stirring of the TiO_2-bacterial suspensions of *E. coli K12* obtained from the *Deutsche Sammlung von Mikroorganismen und Zellkulturen GmbH* (DSM, Cat No. 23716).

2.2. Bacterial strain and growth media

The bacterial strain *E. coli* K12 was inoculated into the nutrient broth No. 2 (N. Oxoid 2, Switzerland) and grown overnight at 37 °C by constant agitation under aerobic conditions. The bacterial growth was monitored at 600 nm by optical means. At an exponential growth phase of 0.8 (as detected at λ = 600 nm) bacterial cells were collected by centrifugation using 500 × *g* for 10 min at 4 °C. Subsequently the bacterial pellet was washed three times by with tryptone solution. The initial solution had cell density of 2.5×10^7 colony-forming *E. coli* units per milliliter (CFU/ml). Cell suspensions were diluted in tri-distilled water in Pyrex bottles of 50 ml to the required cell density, corresponding to 10^4–10^7 colony forming units per milliliter (CFU/ml). Serial dilutions were prepared in tryptone solution and the samples plated on agar Plate-Count-Agar (PCA, Merck, Germany). Other details of the bacterial survival kinetics have been published recently [5].

2.3. Attenuated total reflection Fourier transform spectroscopy

The ATR-FTIR spectra were measured in a Portmann Instruments AG spectrophotometer equipped with a Specac attachment (45° one pass diamond crystal). Spectra were the results of 256 scans with a resolution of 2 cm^{-1} in the spectral range 4000–500 cm^{-1}. Specimens for ATR-FTIR were prepared by two different techniques: (1) 0.5 ml of the liquid from the batch reactor was evaporated on the microscope glass, and (2) 5 ml of the liquid from the reactor was filtered by a MILLIPORE® 0.22 μm filter. Specimens containing the organic moiety and the TiO_2 slurry were contacted with diamond crystal and then the ATR-FTIR spectrum was taken. Both methods showed similar results.

2.4. Transmission electron microscopy

TEM observations were performed on a Philips CM 300 UT/FEG microscope fitted with a Shottky field emission gun operated at 300 kV and with an objective lens with a very short spherical aberration coefficient (0.65 nm).

2.5. Atomic force microscopy

A nanoscope multimode scanning probe microscope (SPM, Digital Instruments Inc., USA) was used for the AFM measurements. Single beam silicon nitride probes (D) NP-S with spring constant 0.58 N/m was used to perform the experiment. Applied force, *F* = 1.5 V; scan rate = 1.5 Hz. The samples for the AFM images were prepared: the 100 μl *E. coli* mixed with the TiO_2 slurry was dropped on the glass and dried.

3. Results and discussion

3.1. ATR-FTIR spectra of E. coli during photocatalysis and deconvolution procedures

Fig. 1 shows the ATR-FTIR spectra in the range of 1800–900 cm^{-1} of the *E. coli* as a function of photocatalysis time is shown in the Fig. 1. The ATR-FTIR peaks of an *E. coli* before irradiation are assigned to: (1) bands at 1645 cm^{-1} (amide I) arising principally from ν(C=O) stretching vibrations; (2) bands at 1540 cm^{-1} (amide II) due primarily to N–H bending with contributions from the C–N stretching vibrations of the peptide group. A water absorption peaks was observed at 1634 cm^{-1}. The bands around 1280–1200 cm^{-1} arise from the nucleic acids bands [6] overlapping with the asymmetric stretching mode $\nu_{as}(PO_2^-)$of the phospholipid phospho-diester and with the non-stoichiometric lipopolysaccharides PO_2^- (LPS). The peaks between 1200 and 950 cm^{-1} are due to the vibrations of the sugar rings of LPS and also to sugar rings from other cell moieties such as: peptidoglycan and exo-polysaccharides (EPS), sometimes labeled capsular polysaccharides (CPS) [3,4,6–12]. The EPS major components of the slime and CPS present a strong chemical similarity to the polysaccharide component of LPS [13].

Fig. 1B shows the Fourier deconvolution of the spectral profiles presented above in Fig. 1A. The deconvolution procedure was used to enhance the resolution of the overlapping bands reported in Fig. 1B. The procedure employed allows the detailed discrimination of the overlapping peaks for: (1) the amide I bands which could be resolved into the individual peaks at 1654, 1635 cm^{-1}; (2) the $-CH_2$ scissor vibration found at 1468 cm^{-1}; (3) the peaks of the ν(C=O) carbonyl vibrations of the wall lipids at 1734 and 1711 cm^{-1}; (4) the peaks of 1153.4, 1117.4, 1102, 1058, 993.45 and 966.36 cm^{-1} which coincide with the peaks reported for ν(C–O) ring, ν(C–O), ν(C–C), and the δ(COH) vibrations of carbohydrates [14]. The region of 1120–1140 cm^{-1} relates to ν_{as}(C–O–C) glycosidic linkage [13]; (5) the 1240 and 1218 cm^{-1} peaks correspond to the absorbance region of nucleic acids. The peak of 1085 cm^{-1} matches the assignment for the $\nu_s(PO_2^-)$ phosphate band of DNA [3].

As it can be seen from Fig. 1 The ATR-FTIR spectra of *E. coli* vary during the photocatalytic treatment in the fingerprint region with time and it was observed that:

(1) The profile of polysaccharide bands were observed to change significantly during irradiation. In the ν_{as}(C–O–C) glycosidic linkage region 1117.5 cm^{-1} and 1102 cm^{-1} bands disappear and new band 1120 cm^{-1}

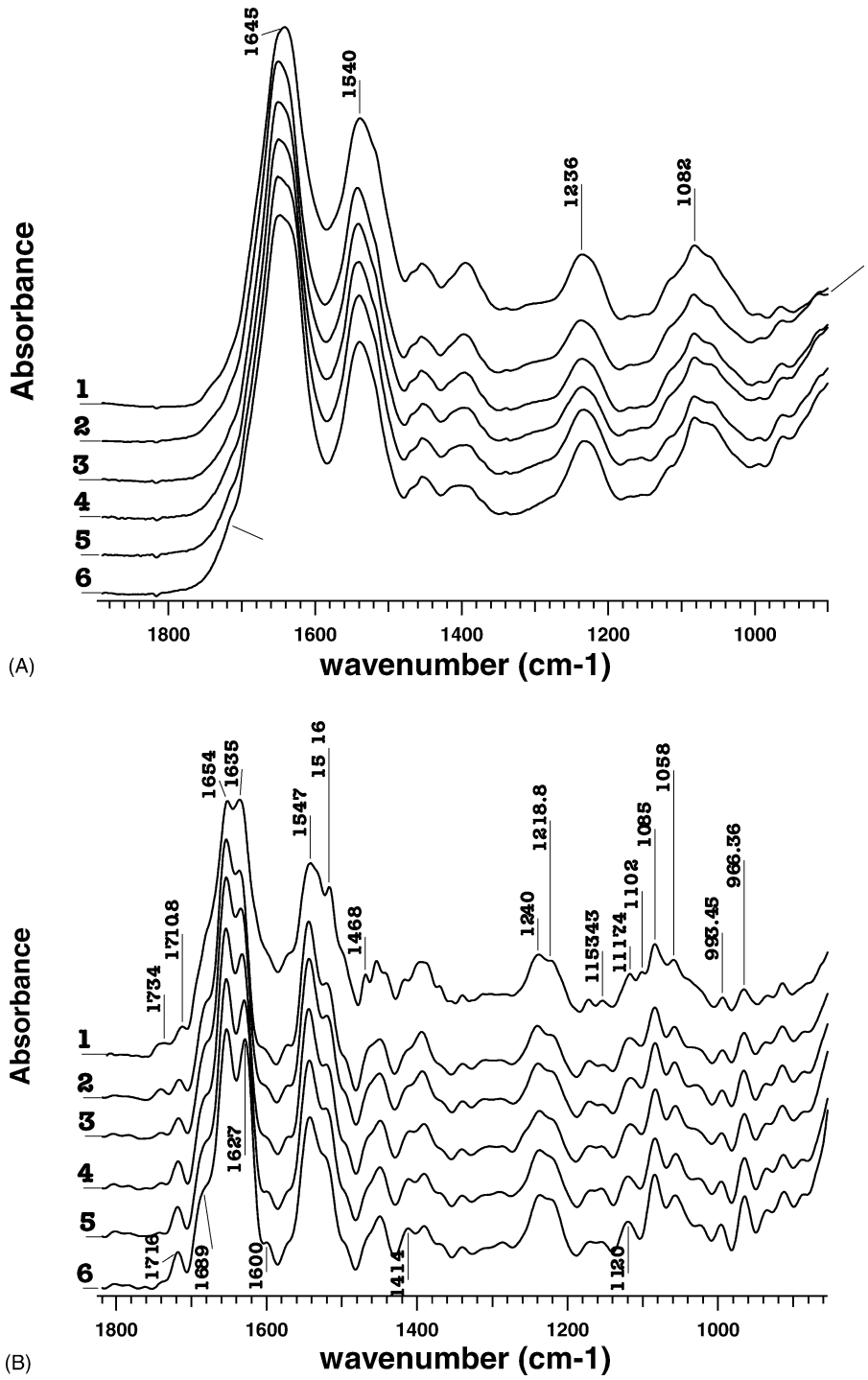

Fig. 1. ATR-FTIR spectra of *E. coli* after different irradiation times in the presence of TiO_2 Degussa P-25 (1 mg/ml). (A) *E. coli* spectra without mathematical treatment. (B) Deconvolution of the spectra with parameters $K = 1.774$ (K is defined as the effective increase in deconvolution), half width = 17.193 cm^{-1}. Spectral profiles were normalized to the maximum at the amide I band. The time of the treatment was: (1) 0 min; (2) 10 min; (3) 20 min; (4) 45 min; (5) 85 min; (6) 150 min.

grows in. The intensity decrease of the broad 1140–1000 cm^{-1} band was detected. The external bilayer of the asymmetric outer membrane is composed only by amphipatic molecules, the lipo-polysaccharides [12,14]. This makes it possible to relate the observed spectral changes to LPS peroxidation during the initial stage of the peroxidation process.

(2) The carbonyl group absorbance between 1800 and 1600 cm^{-1} changed considerably in the ATR-FTIR spectra. A raise in the peak intensities at 1716 cm^{-1} and

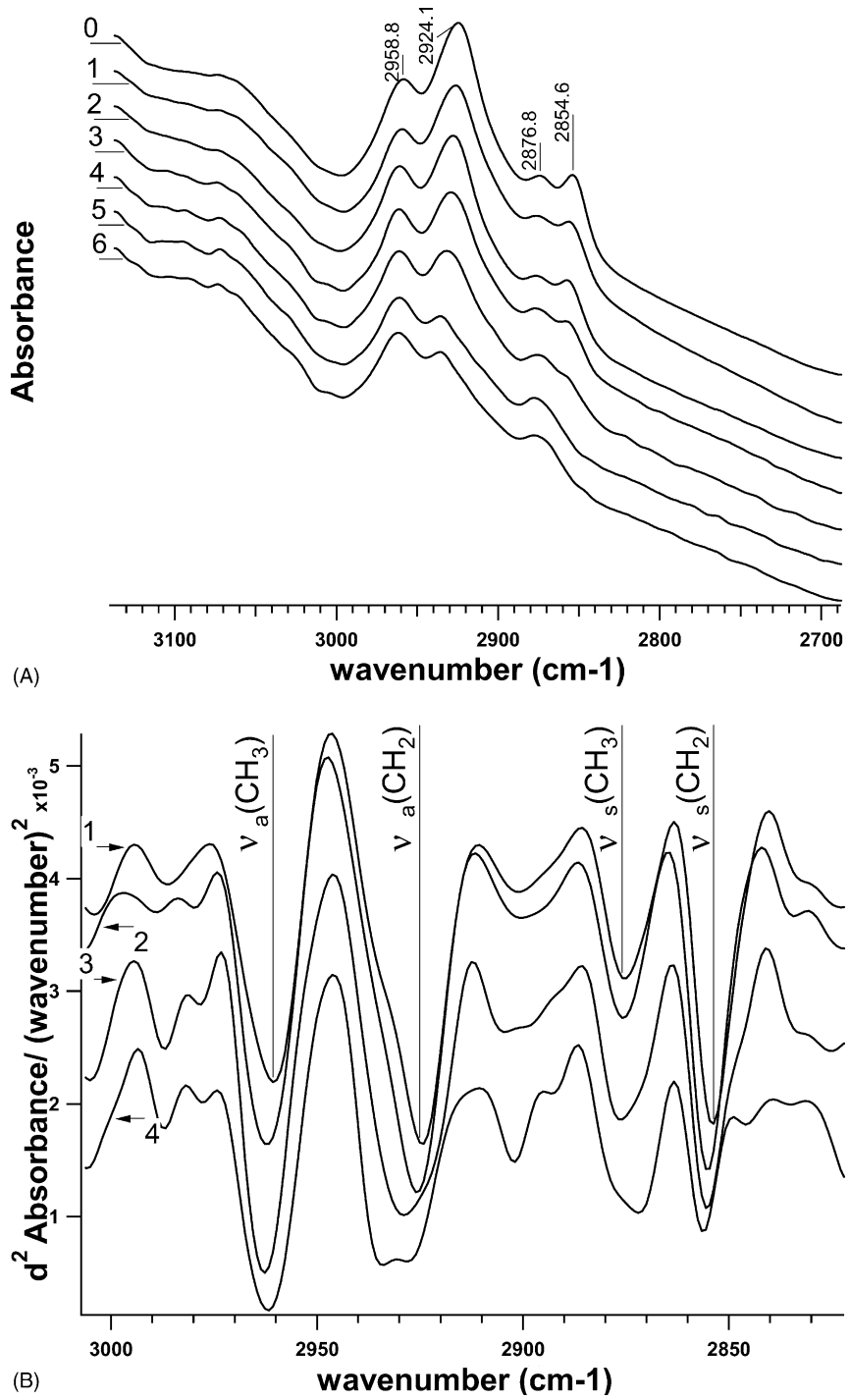

Fig. 2. ATR-FTIR spectra of *E. coli* after different irradiation times in the presence of TiO_2 Degussa P-25 (1 mg/ml). The focus is on the –CH vibrational absorbance region. (A) *E. coli* spectra profiles. (B) Second derivatives of the spectra profiles. In (A) and (B) the irradiation times are: (0) *E. coli* without TiO_2 control spectrum after 85 min illumination. The time of treatment for *E. coli* in the presence of TiO_2 are: (1) 0 min; (2) 10 min; (3) 20 min; (4) 45 min; (5) 85 min; (6) 150 min.

at 1600 cm^{-1} were readily detected. A concomitant increase in the absorption shoulder at 1689 cm^{-1} also occurred. The resolved peaks at 1414 and 1390 cm^{-1} were detected after 150 min peroxidation. These spectral changes have been reported due to the formation of the α,β unsaturated aldehydes during the breakdown of hydroperoxides or lipid endoperoxides and the appearance of C=O stretching bonds during the formation of carboxy-groups [16]. The observed carboxy-group during the oxidation process appears near 1400 cm^{-1} and corresponds to the O=C–O^- symmetric stretching vibrations. The decrease of the peak at

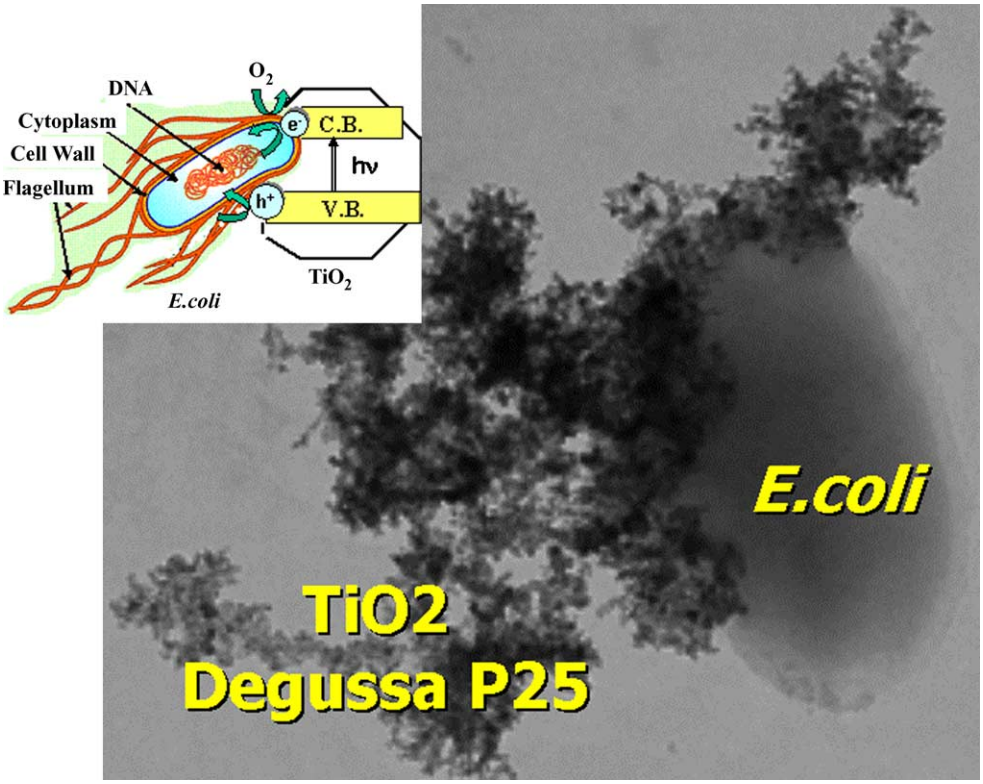

Fig. 3. TEM of a dispersion of TiO_2 Degussa P-25 1mg/l in contact with *E. coli* K-12 cells.

1734 cm^{-1} stands for the breaking of the acyl-bond in lipids.

(3) Significant changes in the profile of PO_2^- bands were observed in the spectral range 1280–1200 cm^{-1}. Band profiles of PO_2^- are sensitive to the hydration–dehydration of the phosphonic groups and this taken as an indicator for the structural organization of lipids [15].

(4) The amide I band(s) were observed to vary during the irradiation in Fig. 1B providing the evidence for the protein conformational changes [3,4]. No changes were detected in the dark after 200 min contact of *E. coli* with TiO_2.

3.2. ATR-FTIR spectra of –CH bands during photocatalysis and deconvolution procedures

Fig. 2 shows the spectra of *E. coli* during the photocatalytic treatment in the presence of TiO_2 in the region 3100–2700 cm^{-1}. The $\nu_a(CH_3)$ vibration bands are shown at 2958.8 cm^{-1}, $\nu_a(CH_2)$ at 2924.08 cm^{-1}, $\nu_s(CH_3)$ at 2876.8 cm^{-1} and $\nu_s(CH_2)$ at 2854.6 cm^{-1}.

The illumination of *E. coli* without TiO_2 slurry and *E. coli* with TiO_2 in dark did not change the spectrum of the –CH bands (Fig. 2A—time 0). The irradiation of *E. coli* with TiO_2 leads to a spectral shift of the peak maximum for the $\nu_s(CH_2)$ peak from 2854.6 to 2856.6 cm^{-1} within 45 min. The observed spectral shift of $\nu_s(CH_2)$ band of about 2 cm^{-1} during the initial stage of the treatment can be attributed to the increase in the lipid-layer fluidity of the *E. coli* cell walls. This structure and fluidity of the LPS monolayer have been reported to be very sensitive to peroxidation in the case of polar-saccharide moieties [12]. Longer treatment times lead to significant changes in the spectral range 3100–2700 cm^{-1}. These changes reflect the deep peroxidation of the *E. coli* lipid-layers.

3.3. Transmission electron microscopy studies

Fig. 3 shows the TEM of a dispersion of TiO_2 Degussa P-25 1 mg/l in contact with *E. coli* K-12 cells. The titania particles at the concentrations used are seen to form aggregates of the basic crystal 20–30 nm. The average size (diameter) obtained for the egg-like *E. coli* (long axis) was seen to be about 1 μm. The surface interaction of TiO_2 with *E. coli* at pH 6 is favored by the fact that *E. coli* is negatively charged between pH 3 and 9 [2]. The *E. coli* surface is negative charged due to polysaccharides of LPS which predominate over the amide (and related positively charged species). This provides an overall negative charge to *E. coli*. Fig. 4 shows the negative bacteria interacting with the positively charged TiO_2 aggregates in aqueous solution. Concomitantly a significant part of the TiO_2 aggregates remains in the solution outside of the field of attraction of the bacterial wall possibly due to the minority positive functional groups on the *E. coli* surface.

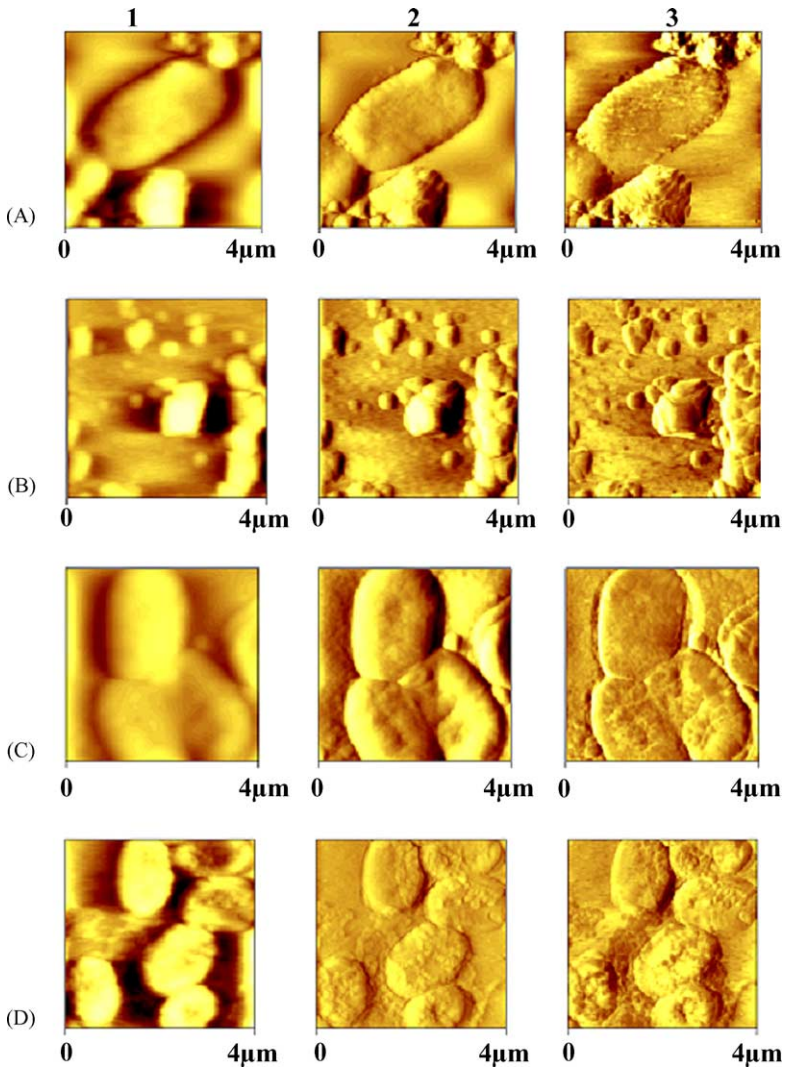

Fig. 4. AFM images of *E. coli* after irradiation with TiO_2 Degussa P25 (1 mg/ml). (A) *E. coli* from TiO_2 slurry before treatment. Column 1 Data type height, *Z* range 1 μm; Column 2 Data type deflection, *Z* range 0.0600 nm; Column 3 Data type friction, *Z* range 15 V. (B) *E. coli* from TiO_2 slurry after 1 h treatment. Column 1 Data type height, *Z* range 800 nm; Column 2 Data type deflection, *Z* range 0.0400 nm; Column 3 Data type friction, *Z* range 10 V. (C) *E. coli* without TiO_2 before illumination. Column 1 Data type height, *Z* range 2 μm; Column 2 Data type deflection, *Z* range 0.0400 nm; Column 3 Data type friction, *Z* range 5 V. (D) *E. coli* without TiO_2 after 1 h illumination. Column 1 Data type height, *Z* range 800 nm; Column 2 Data type deflection, *Z* range 0.15 nm; Column 3 Data type friction, *Z* range 10.1 V.

3.4. AFM and E. coli viability data during TiO_2 mediated photocatalysis

Fig. 4 shows the control AFM micrographs of *E. coli* for (a) non-irradiated control samples in the presence of the TiO_2 slurry and for (b) samples without TiO_2 after 1 h light irradiation. Fig. 4 shows that *E. coli* cells were not detected after 1 h when irradiation were carried out in the presence of TiO_2. In the latter case, the bacterial survival kinetics shows a decrease in the number of cells from 2.5×10^7 CFU/ml at time zero to 8×10^6 CFU/ml after 30 min, to 7×10^5 CFU/ml after 1 h and 10^2 CFU/ml after 2 h irradiation. Control experiments in the absence of TiO_2 but under light irradiation showed a bacterial survival of 2×10^7 CFU/ml after 1 h and 10^7 CFU/ml at 2 h. If the bacterial killing is determined by lysis then the AFM images reported above agree with the survival kinetics showing that the bacteria concentration decreases 35 times within 1 h. Previously in this study the Figs. 1 and 2 have shown that after 1–2 h photocatalysis the *E. coli* proteins, LPS and EPS were not completely oxidized. Figs. 1 and 2 show the functional groups due to low levels of peroxidation, but the peroxidation occurs when the major part of the initial proteins LPS and EPS is still present. Because the *E. coli* in the presence of TiO_2 were not observed by AFM after 1 h irradiation, it is possible to suggest that the lysis of *E. coli* occurs due to damage/changes induced previously in the bilayers of *E. coli*. These changes were seen by ATR-FTIR to involve the appearance of new surface oxidized functional

groups accompanied by a significant shift in the position of –CH groups. This provides proof for the damage occurring in the *E. coli* organized structure and can be considered as the events leading to bacterial lysis.

4. Conclusions

The combination of ATR-FTIR with AFM and viability data have shown to be able during this study to provide the experimental proof for the events leading to *E. coli* photokilling.

This study provides the first evidence by ATR-FTIR spectroscopy into the organized structure of intact and viable *E. coli* membranes without using probe molecules or deuterated fatty acids.

The –CH symmetric stretching ($\nu_s(CH_2)$) band spectral shift during TiO_2 photocataylsis was found to be a valuable tool to monitor the progressive disorder in Gram-negative *E. coli* bacteria as the precursor event of the bacterial lysis.

Acknowledgments

This study was supported by the grants: CTI/KTI TOP NANO-21 No. 5897.5 and OFES COST –19 No. CO2.0068 and INTAS 00-0554. We thank Ph. Buffat from the CIME (EPFL) for his help with the TEM.

References

[1] K. Sunada, T. Watanabe, K. Hashimoto, J. Photochem. Photobiol. A: Chem. 156 (2003) 227.
[2] D.M. Blake, P.C. Maness, Z. Huang, E.J. Wolfrum, J. Huang, W.A. Jacoby, Sep. Purif. Methods 81 (1999) 1.
[3] J.M. Le Gal, M. Manfait, T. Theophanides, J. Mol Struct. 242 (1991) 397.
[4] D. Naumann, Appl. Spectrosc. Rev. 36 (2001) 239.
[5] A.G. Rincoin, C. Pulgarin, Appl. Catal. B, Environ. 44 (2003) 263.
[6] W. Bouhedja, G.D. Sockalingum, P.P. Pina, C. Allouch, R. Bloy, J.M. Labia, M. Millot, Manfait, FEBS Lett. 412 (1997) 39.
[7] D.G. Cameron, H.L. Casal, H.H. Mantsch, Biophys. J. 25 (1979) 289.
[8] W.U. Gorntschelnokow, D. Naumann, C. Weise, F. Hucho, Eur. J. Biochem. 213 (1993) 1235.
[9] C. Parquet, B. Flouret, M. Leduc, Y. Hirota, J. van Heijenoort, Eur. J. Biochem. 133 (1983) 371.
[10] W. Zeroual, C. Choisy, S.M. Doglia, H. Bobichon, J.F. Angiboust, M. Manfait, Biochim. Biophys. Acta—Mol. Cell Res. 122 (1994) 171.
[11] W. Zeroual, M. Manfait, C. Choisy, Pathol. Biol. 43 (1995) 300.
[12] D. Naumann, C. Shultz, A. Sabisch, M. Kastowsky, H. Labischinsi, J. Mol. Struct. 214 (1989) 213.
[13] G. Michael, V. Dupont, A. Dufour, O. Sire, Biochemistry 40 (2001) 11938.
[14] M. Kacurakova, M. Mathlouthi, Carbohydr. Res. 284 (1996) 145.
[15] R. Kinder, C. Ziegler, J.M. Wessels, Int. J. Radiat. Biol. 71 (1997) 561.
[16] A. Gericke, H. Huhnerfuss, Langmuir 11 (1995) 225.